5G-coded fluid antenna multiple access over block fading channels

Hanjiang Hong,[1,✉] Kai-Kit Wong,[1] Kin-Fai Tong,[1] Hao Xu,[1] and Haoyang Li[2]

[1]Department of Electrical and Electronic Engineering, University College London, London, UK

[2]Cooperative Medianet Innovation Center (CMIC), Shanghai Jiao Tong University, Shanghai, China

✉ E-mail: hanjiang.hong@ucl.ac.uk

Fluid antenna multiple access (FAMA) is a concept capable of massive connectivity on the same physical channel without the need of precoding or interference cancellation, by exploiting a super-high dimensional received signal in the spatial domain from fluid antenna system (FAS). This letter investigates the use of 5G New Radio (NR) Modulation Coding Scheme (MCS) for FAMA systems to improve its connectivity over block fading channels. In particular, an iterative decoding receiver with iterative interference covariance estimation is proposed, designed explicitly for slow fading channels. Extrinsic information transfer (EXIT) chart is used to analyze the performance of the proposed iterative receiver. Both EXIT chart analysis and numerical results indicate that the proposed receiver outperforms the existing approach that uses fixed covariance in block fading channels. Also, the results indicate that coded FAMA can serve 100 user terminals (UTs) at the rate of 0.5 bit/s/Hz under rich scattering.

Introduction: The fifth generation (5G) and beyond systems increasingly require multiple access technologies to accommodate many users on the same physical channel [1]. One promising multiple access technology is fluid antenna multiple access (FAMA) [2, 3]. FAMA utilizes the fluid antenna system (FAS) technology [4, 5] for each user, allowing them to operate at the natural interference null. The schemes discussed in [2, 6] are known as *fast* FAMA since they require FAS to switch antenna position on a symbol-by-symbol basis. In contrast, *slow* FAMA, as described in [3, 7, 8], is more practical because it only necessitates antenna position changes when the channel conditions change.

Recently in [9], coded modulation schemes have been considered for fast FAMA, resulting in the *coded* FAMA system, and it was illustrated that connectivity performance can be greatly improved by coding under fast fading. Motivated by this, it is important to see if the same benefits are possible when the channel undergoes slow fading.

In this letter, as in [9], we apply the 5G New Radio (NR) Modulation Coding Scheme (MCS) to slow FAMA and our objective is to study the performance of the coded FAMA system over block fading channels. The *coded* FAMA system adheres to the modulation and channel coding procedures of 5G NR [10], and the robust 5G NR MCS boosts the connectivity of the *coded* FAMA system. However, the state-of-the-art correlated demapper, which utilizes a fixed interference covariance matrix in the iterative decoding receiver in [9], is inadequate for block fading channels, since it does not fully utilize the statistical channel properties to further enhance the performance. To address this limitation, in this design, we propose to estimate the interference covariance matrix iteratively. Both extrinsic information transfer (EXIT) chart and simulation results indicate that the proposed iterative receiver with estimated covariance provides better performance compared to the existing methodology that relies on a fixed covariance. Our simulation results will show that coded FAMA using 5G channel codes can still achieve massive connectivity under block fading channels.

System model: Consider a system in which a base station (BS) communicates to U user terminals (UTs). The BS has U distributed fixed-position antennas, each for sending an information-bearing signal to one UT, while each UT is equipped with a FAS. The information sequences for U UTs are parallel processed with the same MCS. For the u-th UT, the information bit sequence $\boldsymbol{b}^{(u)} = \{b^{(u)}[0], \dots, b^{(u)}[N_b-1]\}$ is encoded as $\boldsymbol{c}^{(u)} = \{c^{(u)}[0], \dots, c^{(u)}[N_c-1]\}$, and then mapped to a symbol sequence $\boldsymbol{s}^{(u)} = \{s^{(u)}[0], \dots, s^{(u)}[N_s-1]\}$. The transmission rate can be easily found as $R = N_b/N_s = mN_b/N_c$, where $m = \log_2 M$, and M is the modulation order.

Each UT's FAS has $N = N_1 \times N_2$ uniformly distributed ports within a physical size of $W_1\lambda \times W_2\lambda$, where λ is the carrier wavelength. For notational simplicity, we map the 2D antenna port indices to a single index: $(k_1, k_2) \to k$, where $k_1 \in \{0, \dots, N_1-1\}$, $k_2 \in \{0, \dots, N_2-1\}$, and $k \in \{0, \dots, N-1\}$. The received signal at the k-th port of UT u can be written as

$$r_k^{(u)}[t] = g_k^{(u,u)} s^{(u)}[t] + \sum_{\substack{\tilde{u}=1 \\ \tilde{u}\neq u}}^{U} g_k^{(\tilde{u},u)} s^{(\tilde{u})}[t] + \eta_k^{(u)}[t], \tag{1}$$

where $t \in \{0, \dots, N_s-1\}$, $g_k^{(\tilde{u},u)}$ denotes the fading channel from the $\tilde{u}$-th BS antenna to UT u at the k-th port, and $\eta_k^{(u)}[t]$ is the zero-mean complex Gaussian noise with variance of σ_η^2. For simplicity, the time index t is omitted in the rest of the letter unless specified otherwise.

We assume that UT u knows its own channel $\{g_k^{(u,u)}\}_{\forall k}$ to retrieve the information symbols from the signals $\{r_k^{(u)}\}_{\forall k}$. With FAS, each user is able to select the antenna port(s) by evaluating the signal-to-noise and interference ratio (SINR) so that

$$k_n^* = \arg \max_{k \backslash \{k_0^*, \dots, k_{n-1}^*\}} \Gamma_k, \; n = 0, \dots, N^*-1, \tag{2}$$

where Γ_k is the instantaneous SINR when considering fast FAMA [2], or the average SINR when considering slow FAMA [3].

In [9], the selected received signals $\boldsymbol{r}^* = [r_{k_0}^{(u)}, \dots, r_{k_{N^*-1}}^{(u)}]^T$ are combined by a correlated demapper. The *extrinsic* log-likelihood ratio (LLR) of the i-th bit b_i of symbol s, $L_e(b_i)$, is given by

$$L_e(b_i) = \ln \frac{\sum_{s \in \chi_i^{(0)}} p(\boldsymbol{r}^*|s) p_a(s)}{\sum_{s \in \chi_i^{(1)}} p(\boldsymbol{r}^*|s) p_a(s)} - L_a(b_i), \tag{3}$$

in which $\chi_i^{(b)}$ denotes the constellation subset with the i-th bit being $b \in \{0, 1\}$, L_a is the a priori LLR, and $p_a(s)$ is the a priori probability. The conditional probability density function (PDF) $p(\boldsymbol{r}^*|s)$ in (3) over the correlated FAS channel is calculated as

$$p(\boldsymbol{r}^*|s) = \frac{1}{\pi^{N^*} |\hat{\boldsymbol{\Sigma}}^*|} \exp\left[-(\boldsymbol{r}^* - \boldsymbol{g}^* s)^\dagger \hat{\boldsymbol{\Sigma}}^{*-1} (\boldsymbol{r}^* - \boldsymbol{g}^* s) \right], \tag{4}$$

where $\boldsymbol{g}^* = [g_{k_0}^{(u,u)}, \dots, g_{k_{N^*-1}}^{(u,u)}]^T$ denotes the channel coefficients of the selected ports, $\hat{\boldsymbol{\Sigma}}^*$ is the covariance matrix of the selected ports. This covariance matrix is derived from the FAS channel correlation $\boldsymbol{\Sigma}$ as

$$\hat{\boldsymbol{\Sigma}}^* = \left[(U-1) E_s \sigma^2 \boldsymbol{\Sigma} + \sigma_\eta^2 \boldsymbol{I} \right]_{\{k^*\}}. \tag{5}$$

Based on the eigenvalue-based FAS channel model [11], the elements in $\boldsymbol{\Sigma}$ under rich scattering are given by

$$[\boldsymbol{\Sigma}]_{k,l} = J_0\left(2\pi \sqrt{\left(\frac{k_1 - l_1}{N_1 - 1} W_1 \right)^2 + \left(\frac{k_2 - l_2}{N_2 - 1} W_2 \right)^2} \right), \tag{6}$$

where $(l_1, l_2) \to l$, and $J_0(\cdot)$ denotes the zero-order Bessel function of the first kind. This correlated demapper with the fixed covariance matrix $\hat{\boldsymbol{\Sigma}}^*$ in (5) performs well in fast fading channels [9]. Still, there is more performance gain to be achieved by exploiting the statistical properties of the channel in block fading channels, as will be shown by simulation results later.

Iterative receiver with interference covariance estimation: In this section, we propose an iterative receiver estimating the interference covariance matrix by iterations. As shown in Figure 1, the iterative receiver consists of the port selector, the interference covariance estimator, the correlated demapper and the decoder. The soft information is transferred between the components in the form of LLR.

In this letter, the port selector chooses the ports by (2) based on the average SINR, that is,

$$\Gamma_k = \frac{\left| g_k^{(u,u)} \right|^2 \mathbb{E}_t \left\{ \left| \tilde{s}_k^{(u)}[t] \right|^2 \right\}}{\mathbb{E}_t \left\{ \left| r_k^{(u)}[t] \right|^2 \right\} - \left| g_k^{(u,u)} \right|^2 \mathbb{E}_t \left\{ \left| \tilde{s}_k^{(u)}[t] \right|^2 \right\}}, \tag{7}$$

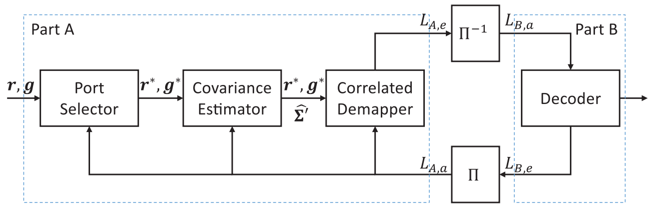

Fig. 1 *The proposed iterative receiver*

where $\hat{s}^{(u)} = \sum_{s\in\chi} s \cdot p_a(s)$ is the expectation calculated based on the a priori probability $p_a(s)$. In the initial process, the a priori $p_a(s)$ is assumed equally likely, that is, $p_a(s) = 1/M$. From the second pass, the *extrinsic* LLR $L_{A,e}$ is interleaved and feedback as a priori information $L_a = L_{B,a}$ of the demapper, and the a priori $p_a(s)$ is calculated as

$$p_a(s) = \prod_{i=0}^{m-1} \frac{\exp\left[(1-b_i)L_a(b_i)\right]}{1+\exp L_a(b_i)}. \tag{8}$$

The interference covariance matrix of the selected ports can be estimated based on the a priori expectation symbol $\hat{s}^{(u)}$ as

$$\hat{\boldsymbol{\Sigma}}' = \frac{1}{N_s}\sum_{t=1}^{N_s} (\boldsymbol{r}^*[t] - \boldsymbol{g}^*\hat{s}^{(u)}[t])(\boldsymbol{r}^*[t] - \boldsymbol{g}^*\hat{s}^{(u)}[t])^\dagger. \tag{9}$$

The correlated demapper then uses (9) to calculate the PDF in (4) and the LLR in (3), and transferred to the decoder.

The receiver's complexity increases because of the additional interference covariance matrix estimation process. The complexity of this estimation is $\mathcal{O}\left(N_s \times (N^*)^2\right)$, which is determined by the number of multiplication operations in (9). This complexity is much lower than the overall demapping complexity of $\mathcal{O}\left(N_s \times M \times (N^*)^2\right)$ [9], where M is the modulation order. Thus, the complexity overhead is considered acceptable.

EXIT chart: EXIT chart [12] uses the mutual information between the LLRs and the transmitted bits to model the transfer behavior of each component in the iterative receiver. In our analysis, the receiver is divided into Part A and Part B, as depicted in Figure 1. Part A includes the port selector, the interference covariance estimator, and the correlated demapper, while Part B is the decoder. The transfer function of Part A can be expressed as $I_{A,e} = T_A(I_{A,a}, \hat{\boldsymbol{\Sigma}}')$. However, it is difficult to derive a closed form of either T_A or Part B's transfer function T_B. Monte-Carlo simulations are used to calculate the two functions.

In the case of T_A, we model the a priori LLR $L_{A,a}$ as an independent zero-mean Gaussian random variable n_A having a variance of σ_A^2, in conjunction with input bits $b \in \{0,1\}$ or equivalent $x \in \{-1,+1\}$, that is, $L_a = \sigma_A^2/2 \cdot x + n_A$. The variance σ_A^2 is given by $\sigma_A = J^{-1}(I_{A,a})$, where the function $J(\sigma)$ is defined as

$$J(\sigma) \triangleq I_A(\sigma_A = \sigma)$$

$$= 1 - \frac{1}{\sqrt{2\pi}\sigma}\int_{-\infty}^{+\infty} \exp\left[-\frac{\left(\zeta - \frac{\sigma^2}{2}\right)^2}{2\sigma^2}\right] \cdot \log_2(1+e^{-\zeta})\mathrm{d}\zeta. \tag{10}$$

Then the a priori LLR $L_{A,a}$ is applied in the port selector, the covariance estimator, and the correlated demapper in Part A to calculate the *extrinsic* LLR $L_{A,e}$, and $I_{A,e}$ is calculated as

$$I_{A,e} = 1 - \mathbb{E}_x\left\{\log_2[1 + e^{-x \cdot L_{A,e}}]\right\}. \tag{11}$$

With over 10,000 independent channel realizations, the EXIT chart of 5G NR MCS 7 (defined in [10], Table 5.1.3.1-1) is shown in Figure 2. The UT's FAS configuration is $N = 6 \times 6$ over the physical size of $2\lambda \times 2\lambda$. MCS 7 uses Quadrature Phase Shift Keying (QPSK) modulation and LDPC code with target code rate of 526/1024, so the transmission rate is about 1.0 bit/s/Hz. Observe in Figure 2 that the proposed Part A demapper with estimated covariance matrix in (9)

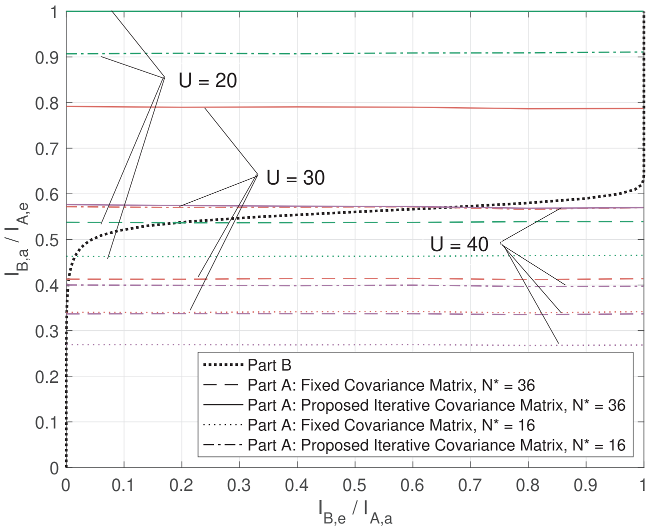

Fig. 2 *EXIT chart of the iterative receiver with the 5G NR MCS 7, while transmitting over rich scattering Rayleigh fading channels with the normalized physical size $W = 2 \times 2$*

provides higher $I_{A,e}$ than the demapper with fixed covariance matrix in (5). Furthermore, $I_{A,e}$ increases when the number of UTs U decreases or when the number of the selected ports N^* increases. Ideally, in order to exchange the extrinsic information between Part A and Part B to achieve a low error rate, the EXIT curve of Part A and the extrinsic EXIT curve of Part B should not intersect before reaching the (1.0,1.0) point. Figure 2 demonstrates that when ($U = 20$, $N^* = 36$ or $N^* = 16$) or ($U = 30$, $N^* = 36$), the EXIT chart of Part A with estimated covariance matrix (9) can provide this *open-convergence tunnel*. But even when $U = 20$, the demapper with (5) cannot achieve the *open-convergence tunnel*. According to the predictions of EXIT charts, the coded FAMA system with the FAS configuration of ($N = 6 \times 6$ over $W = 2 \times 2$) is able to support between 30 and 40 users when $N^* = 36$, and between 20 and 30 users when $N^* = 16$ at the transmission rate of 1.0 bit/s/Hz for each user, with the proposed receiver.

Simulation results: This section presents the block error rate (BLER) results to study the performance of the coded FAMA with the proposed receiver over block fading channels. Channel coding in 5G NR [10], including the block segmenting, the cyclic redundancy check (CRC) encoding, the low-density parity-check (LDPC) encoding, and the rate matching, is considered, and the number of resource elements is $N_{\mathrm{RE}} = 936$. MCS 7 with the transmission rate 1.0 bit/s/Hz and MCS 3 with the transmission rate 0.5 bit/s/Hz are considered [10]. QPSK modulation is used, while LDPC codes with target code rate of 251/1024 and 526/1024 are used in MCS 3 and 7, respectively. Again, rich-scattering Rayleigh fading channels based on the eigenvalue-based FAS channel [11] are considered from each transmit BS antenna to the UT, and all the users are assumed statistically identical and independent.

In Figure 3, we have the BLER results of coded-FAMA with the proposed estimated and the fixed covariance matrix against the number of the fluid antenna ports $N = N_1 \times N_2$, when the normalized physical size is $W = 5 \times 5$. We set different numbers of selected ports N^* for different U, since the connectivity ability increases with N^*. The performance of the proposed estimated covariance matrix in (9) is better than that of the fixed covariance matrix in (5). Also, we see that the error rate decreases with the number of antenna ports N. However, an error floor exists when N is large, because of the correlation between the antenna ports.

The results in Figure 4 study the BLER performance against the normalized physical size $W = W_1 \times W_2$, when $N = 20 \times 20$. As we can see, when N is large enough, a larger FAS size provides better performance. Nonetheless, the BLER saturates when $W > 5 \times 5$. This indicates that further gain may need a larger N when $W > 5 \times 5$.

The BLER performance of the coded FAMA system against the number of selected ports N^* is analyzed in Figure 5. The configuration of FAS at UT is $N = 20 \times 20$ antenna ports over the normalized physical size of $W = 5 \times 5$. We observe that the performance improves when

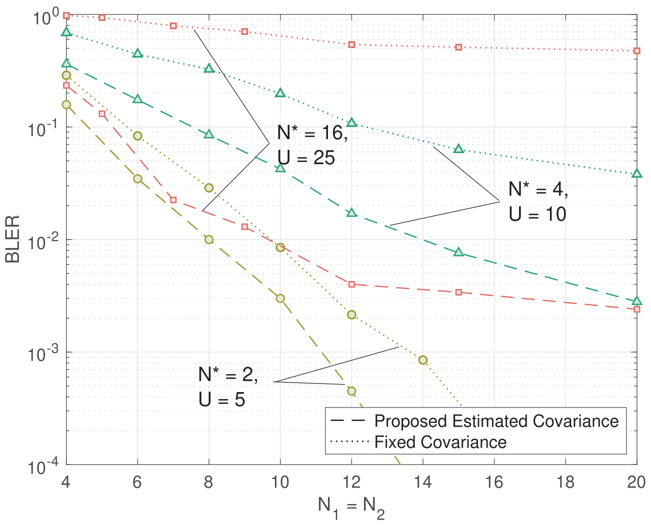

Fig. 3 *The BLER performance of MCS 7 against the number of antenna ports* $N = N_1 \times N_2$*, when* $W = 5 \times 5$

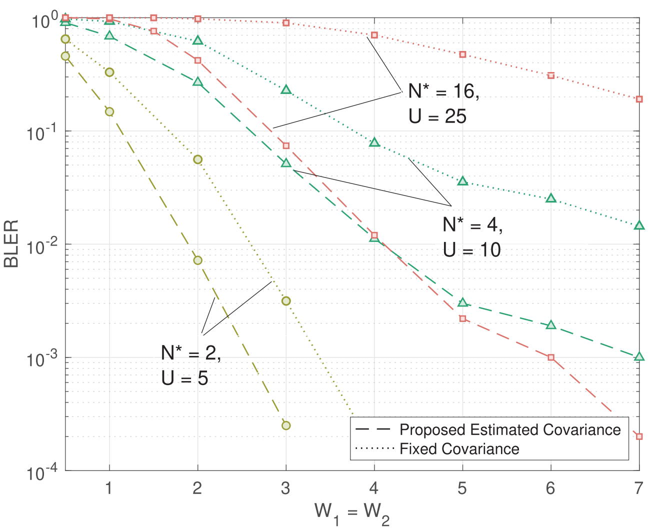

Fig. 4 *The BLER performance of MCS 7 against the nomarlized FAS physical size* $W = W_1 \times W_2$*, when* $N = 20 \times 20$

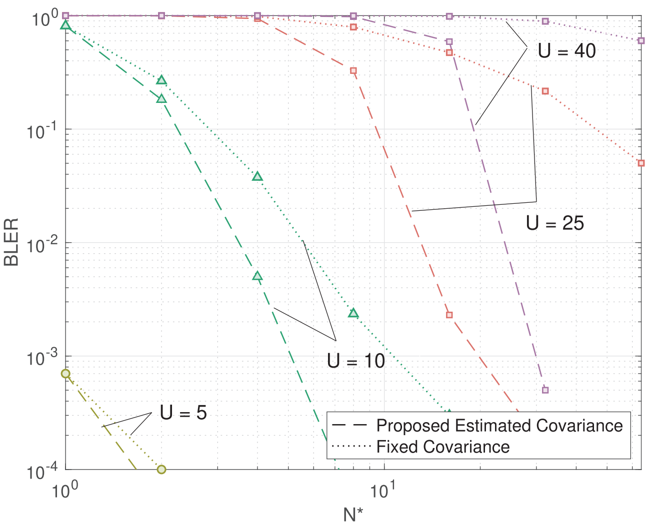

Fig. 5 *The BLER performance of MCS 7 against the number of selected ports* N^**, when* $W = 5 \times 5$ *and* $N = 20 \times 20$

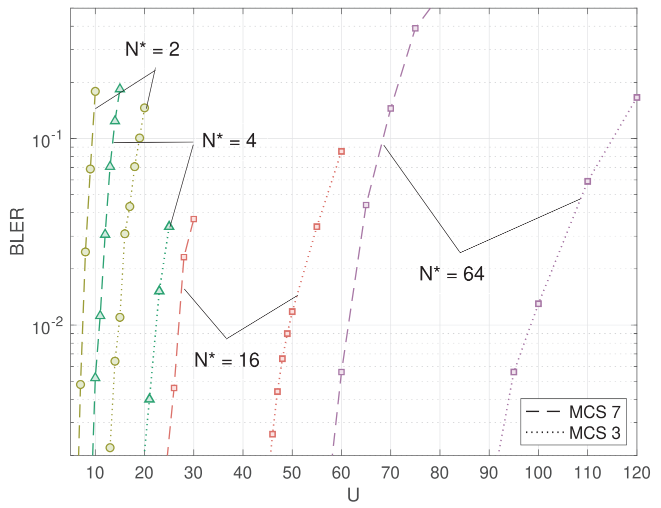

Fig. 6 *The BLER performance of the receiver with the estimated covariance matrix against the number of UTs* U*, when* $W = 5 \times 5$ *and* $N = 20 \times 20$

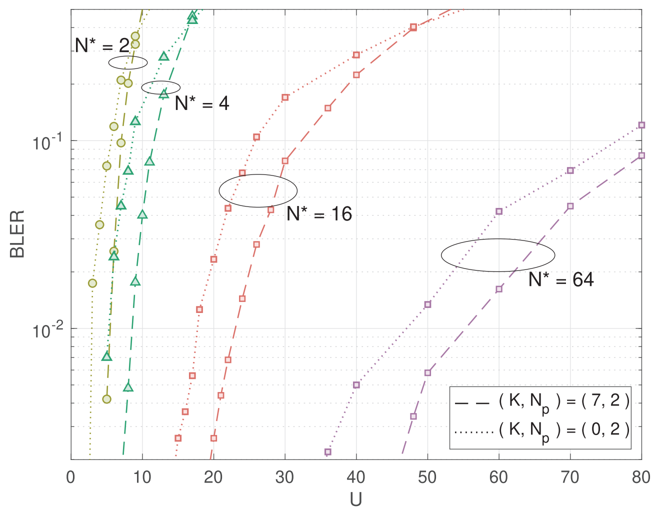

Fig. 7 *The BLER performance of MCS 3 against the number of UTs* U *over finite-scattering channels, when* $W = 5 \times 5$ *and* $N = 20 \times 20$

the number of selected ports N^* is larger. Moreover, with the fixed FAS configuration, the performance of larger connectivity (larger number of users U) is inferior. When $N^* = 16$, realiable transmission can be achieved for $U = 25$ UTs with the threshold of BLER $= 10^{-2}$.

In Figure 6, the results are provided to evaluate the BLER against U considering the same FAS configuration as in Figure 5. We are interested in the largest number of UTs U when BLER is lower than the threshold 10^{-2}. As we can see, the connectivity capability is higher when the number of selected ports N^* is higher, and when the MCS is lower (in which case the channel coding is more robust). A remarkable performance is observed in the case of $N^* = 64$, where nearly 100 UTs can be served simultaneously with a 0.5 bit/s/Hz rate, and more than 60 UTs can be supported with a 1.0 bit/s/Hz rate.

Finally, we evaluate the BLER performance under the finite-scatterer channel model [8] in Figure 7 against U of MCS 3, considering two channel scenarios $(K, N_p) = (0, 2)$ and $(K, N_p) = (7, 2)$ where K is the Rice factor and N_p is the number of scattered paths. The FAS configuration remains the same as in Figure 6. As expected, the performance of the finite-scatterer channel is not as good as that of the rich-scattering case. But the system can still achieve the connectivity of nearly 50 users at the rate of 0.5 bit/s/Hz rate, when $N^* = 64$.

Conclusion: In this letter, we applied 5G NR MCS to obtain a coded FAMA system and studied it for block fading channels. We proposed an iterative decoding receiver that employed an iterative interference covariance estimation to improve the overall performance. EXIT chart analysis and numerical BLER simulation results demonstrated significant connectivity capabilities of coded FAMA over block fading channels. The results revealed that coded FAMA is capable of supporting nearly 100 UTs on the same physical channel with a reasonable configuration of FAS and $N^* = 64$ active selected ports for each user.

Author contributions: **Hanjiang Hong**: Data curation; investigation; methodology; writing—original draft. **Kai-Kit Wong**: Conceptualization; supervision; writing—review and editing. **Kin Fai Tong**: Conceptualization; supervision. **Hao Xu**: Investigation; methodology. **Haoyang Li**: Methodology; writing—review and editing.

Acknowledgements: The work of K. K. Wong and K. F. Tong is supported by the Engineering and Physical Sciences Research Council (EPSRC) under Grant EP/W026813/1. The work of H. Hong is supported by the Outstanding Doctoral Graduates Development Scholarship of Shanghai Jiao Tong University.

Conflict of interest statement: The authors declare no conflicts of interest.

Data availability statement: The data that support the findings of this study are available from the corresponding author upon reasonable request.

Received: *18 November 2024* Accepted: *22 January 2025*
doi: 10.1049/ell2.70166

References

1 Chen, X., Ng, D.W.K., Yu, W., et al.: Massive access for 5G and beyond. *IEEE J. Select. Areas Commun*. **39**(3), 615–637 (2021)

2 Wong, K.K., Tong, K.F.: Fluid antenna multiple access. *IEEE Trans. Wireless Commun.* **21**(7), 4801–4815 (2022)

3 Wong, K.K., Morales-Jimenez, D., Tong, K.F., et al.: Slow fluid antenna multiple access. *IEEE Trans.Commun*. **71**(5), 2831–2846 (2023)

4 Wong, K.K., Tong, K.F., Shen, F., et al.: Bruce Lee-inspired fluid antenna system: Six research topics and the potentials for 6G. *Front. Commun. Netw.* **3**, 853416 (2022)

5 New, W.-K., Wong, K.K., Xu, H., et al.: A tutorial on fluid antenna system for 6G networks: Encompassing communication theory, optimization methods and hardware designs. arXiv preprint, arXiv:2407.03449 (2024)

6 Wong, K.K., Tong, K.F., Chen, Y., Zhang, Y.: Fast fluid antenna multiple access enabling massive connectivity. *IEEE Commun. Lett.* **27**(2), 711–715 (2023)

7 Wong, K.K., Chae, C.B., Tong, K.F.: Compact ultra massive antenna array: A simple open-loop massive connectivity scheme. *IEEE Trans. Wireless Commun.* **23**(6), 6279–6294 (2024)

8 Wong, K.K., Tong, K.F., Chen, Y., Zhang, Y.: Extra-large MIMO enabling slow fluid antenna massive access for millimeter-wave bands. *Electron. Lett.* **58**(25), 1016–1018 (2022)

9 Hong, H., Wong, K.-K., Tong, K.F., et al.: Coded fluid antenna multiple access over fast fading channels. *IEEE Wireless Commun. Lett.* submitted.

10 3GPP TS 38.212 V18.2.0 (2024-03). Technical Specification. https://www.3gpp.org/ftp/Specs/archive/38_series/38.212/38212-i20.zip (2024). Accessed 29 March 2024.

11 Khammassi, M., Kammoun, A., Alouini, M.S.: A new analytical approximation of the fluid antenna system channel. *IEEE Trans. Wireless Commun.* **22**(12), 8843–8858 (2023)

12 El-Hajjar, M., Hanzo, L.: EXIT charts for system design and analysis. *IEEE Commun. Surv. Tutor.* **16**(1), 127–153 (2014)